Laser-induced electron emission from nanostructures: A first-principles study

Joseph A. Driscoll, Sergiy Bubin, and Kálmán Varga
Department of Physics and Astronomy, Vanderbilt University, Nashville, Tennessee 37235, USA
(Received 16 February 2011; revised manuscript received 27 April 2011; published 13 June 2011)

Time-dependent density functional theory simulation of laser-induced ionization is presented. Various test systems including a small wire-like molecule, $C_{12}H_{14}$, as well as carbon nanotubes with varying diameter are studied. It has been demonstrated that significant ionization electron current is produced when a laser pulse is applied. Moreover, pulse-like patterns of the current have been observed, which suggests that short laser pulses can be used to create spatially and temporally localized electron sources.

DOI: 10.1103/PhysRevB.83.233405 PACS number(s): 78.67.Ch, 73.63.Fg, 78.47.−p, 79.70.+q

The rapid development of experimental techniques, especially the advances of high-power femtosecond lasers, allows the investigation of dynamical processes in nanostructures on the subfemtosecond time scale.[1–7] To gain physical insight into the interaction between lasers and nanostructures, the understanding of nanoscale electron dynamics in time-varying fields is needed. Experiments have shown laser-induced ionization in metallic needle cathodes with nanometer-scale sharpness, and is used to generate bright, low-emittance, and short electron bunches with durations down to the femtosecond range, ideal for applications such as time-resolved electron microscopy, compact free-electron lasers,[8] or scanning probe microscopy.[9]

In order for electrons to escape a material and be emitted, they must somehow move beyond the material's confining potential barrier. Lasers can ionize a structure in several ways. If the laser's electric field is able to bend down the confining potential, electrons can tunnel from the material into the vacuum. This is called the field emission regime. When this bending is extreme, such that the top of the tunneling barrier is below the Fermi level of the confined electrons, we have "above barrier" ionization. If the barrier height is oscillating, due to the oscillation of a laser's electric field, for example, tunneling will only be enhanced during the times that the barrier is low. This is called optical field emission.

Electrons can absorb photons to be excited to higher energy states within the potential. If the potential has been bent down by an electric field, the electrons will have enhanced tunneling compared to electrons without photon absorption. This process is called photofield emission. If the potential is not bent down, electrons can still escape via multiphoton absorption, in which the electrons gain enough energy from photons to overcome the confining potential.

The Keldysh parameter $\gamma = \sqrt{8\pi^2\epsilon_F m_e c^2}/\lambda e E$[10] is a quantity that indicates which ionization regime is dominant. Here ϵ_F is the Fermi energy of the electrons in the material, while m_e and e are the mass and charge, respectively, of the electron. λ and E are the wavelength and electric field amplitude, respectively, of the laser. In the photon absorption regime $\gamma \gg 1$, while the "over barrier" case is indicated by $\gamma \ll 1$. If $\gamma \approx 1$, the tunneling regime is dominant.

Theoretical works on description of laser-induced electron emission are in a developmental stage. Simple one-dimensional potential model calculations[1] are used to illustrate the effect of laser pulses on the potential barrier. Other theoretical work includes ultrashort (delta function like) laser pulses ionizing quantum wells,[11] models of Coulomb explosion for nanoscale systems,[12–14] and studies of ionization of small molecules in intense laser fields.[15–17] To see the relative importance of the ionization mechanisms and to understand the highly nonlinear and nonequilibrium laser-induced electron pulses, first-principle calculations are needed.

In this work, we study laser-induced electron emission using time-dependent density functional theory (TDDFT).[18] The TDDFT framework is known[19] to be able to calculate ionization properties for a wide range of laser intensities, from the multiphoton and tunneling[20] regimes to above-threshold ionization.[21] We will show that significant ionization electron current is produced when a laser field is applied. We will also demonstrate that short laser pulses can be used to create spatially and temporally localized electron sources.

The calculations are carried out in real space and real time. The system is placed in a static electric field along with a time-dependent laser field and the Kohn-Sham orbitals are time propagated. From these orbitals, the emitted current is calculated far from the emitter.

TDDFT provides a powerful approach for simulations of interaction of materials and lasers.[22–25] In TDDFT, the evolution of single-particle Kohn-Sham orbitals, ψ_k, is described by a time-dependent equation:

$$i\hbar\frac{\partial\psi_k(\mathbf{r},t)}{\partial t} = H_{\mathrm{KS}}\psi_k(\mathbf{r},t), \tag{1}$$

with the Kohn-Sham Hamiltonian,

$$H_{\mathrm{KS}} = -\frac{\hbar^2}{2m}\nabla^2_{\mathbf{r}} + V_{\mathrm{ion}}(\mathbf{r},t) + V_{\mathrm{H}}[\rho](\mathbf{r},t) + V_{\mathrm{xc}}[\rho](\mathbf{r},t) + V_{\mathrm{ext}}(\mathbf{r},t),$$

where V_{ion} is the ionic potential, V_{H} is the Hartree potential, V_{xc} is the exchange-correlation potential, and V_{ext} is the potential due to an external field. The time-dependent electron density is defined as $\rho(\mathbf{r},t) = \sum_k^{N_{\mathrm{occ}}} f_k|\psi_k(\mathbf{r},t)|^2$, where N_{occ} is the number of occupied Kohn-Sham orbitals and f_k is the occupation of the kth orbital.

For the exchange-correlation potential, we used the adiabatic local density approximation (ALDA), with the parametrization of Perdew and Zunger.[26] The limitations and advantages of the ALDA are discussed in Ref. 23 and it has been demonstrated that the ALDA provides a reasonably good approximation for many-electron ionization in strong fields.

To represent the ionic potential, the pseudopotential approach by Troullier and Martins[27] was employed. For a static electric field applied along the positive x-axis, the potential is $V_{\text{stat}}(x) = -E_{\text{stat}}x$. We include a laser pulse field with the following time-dependent potential:

$$V_{\text{laser}}(\mathbf{r},t) = V_{\text{laser}}(\mathbf{r}) \exp\left[\frac{-(t-t_{\text{peak}})^2}{a^2}\right] \cos(\omega t).$$

Here ω is the laser frequency and $V_{\text{laser}}(\mathbf{r})$ is the amplitude of the oscillating potential. Parameter a controls the width of the Gaussian envelope. We use short laser pulses consisting of just a few oscillations of the electric field. Accordingly, the value of parameter a was 1.7 fs, and the peak of the pulse occurred at $t_{\text{peak}} = 5$ fs.

Since the wavelength of the laser we used (266 nm) greatly exceeds the size of the system, we consider the electric field uniform within the simulation box. Assuming that the laser is linearly polarized along the x axis, $V_{\text{laser}}(x) = -E_{\text{laser}}x$. The direction of a laser's electric field oscillates, and so equal amounts of current could be expected in both the $+x$ and $-x$ directions, yielding a zero net current. For this reason, we also apply a small static electric field. This field is oriented such that a small bias is produced, leading to a preferred direction $(+x)$ for current, and therefore a nonzero net current. Our calculations used $E_{\text{laser}} = 1$ V/Å for all simulations in which the laser was active, and the static field was 0.1 V/Å. This magnitude of the electric field is easily achievable in experiment. In terms of the Keldysh parameter, this laser field corresponds to $\gamma = 5$. This shows that the main ionization mechanism is tunneling, but multiphoton ionization is also possible.

We use a real-space grid to represent quantities, which is a natural choice since electron density moves far from atomic centers. The time-dependent Kohn-Sham equation is solved by propagating the orbitals in time, using the system ground state as the initial state. The full time propagation interval $[t_{\text{init}},t_{\text{final}}]$ is split into N_{step} small steps of length Δt, so that the time evolution operator, $U(t_{\text{final}},t_{\text{init}})$, that acts on the Kohn-Sham orbitals, can be approximated by the product $U(t_{\text{final}},t_{\text{init}}) = \prod_{m=1}^{N_{\text{step}}} U(t_m + \Delta t, t_m)$, where $U(t_m + \Delta t, t_m) = \exp[-i\hat{H}(t_m)\Delta t]$ and t_m is the initial time for the mth step. The electronic density and the Hartree, exchange-correlation, and external field potentials are updated each time step. To approximate the exponential operator, a fourth-order Taylor expansion is used.

In Fig. 1, we show a typical snapshot of the electron density difference (between the initial state of the system and the state at time t) obtained in calculations with a static field only. This figure shows the three-dimensional nature of the density of the emitted electrons and illustrates the need for large simulation cells and absorbing potentials. Since the calculations involve long simulation times, one must avoid reflections from the boundaries of the simulation volume. For this, we use complex absorbing potentials (CAPs).[28,29] In the CAP approach, the amplitude of the wave function outside of the interaction region (i.e., away from the molecule) is effectively attenuated, while the wave function inside the interaction region is unchanged. Many forms of CAPs exist; here we adopt the form described by Manolopoulos.[29]

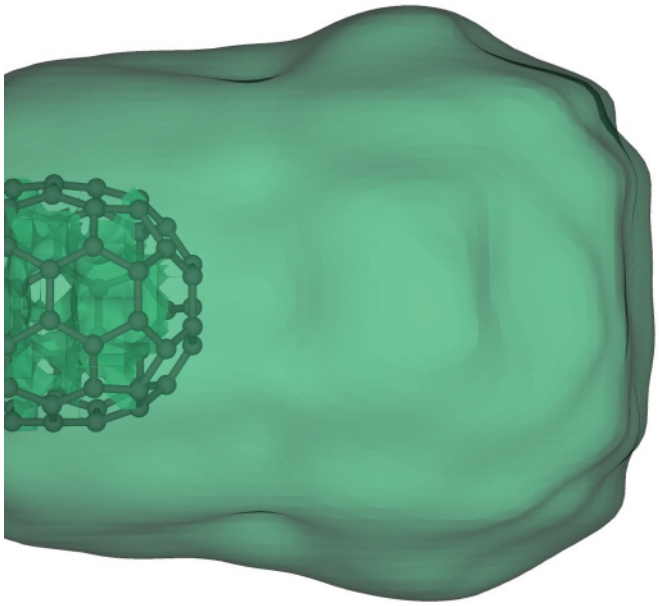

FIG. 1. (Color online) Surface plot of the difference between the electron density at $t = 0$ and 1.2 fs for the case of a (5,5) carbon nanotube and a static electric field.

As test systems, we have used carbon nanotubes and a chain-like molecule, $C_{12}H_{14}$. Figure 2 shows the setup of the calculations. The system under study, in this case a $C_{12}H_{14}$ molecule, is placed in a large simulation box. Both electric fields (i.e., static and laser) are applied along the x axis. Due to the chosen direction of the static electric field, the net flow of electrons will be in the $+x$ direction. This static field is too weak to significantly contribute to the emitted current magnitude. It is present only to provide a small bias, leading to a preferred direction (i.e., $+x$) for the emitted current.

We calculate the current through a plane located at some distance (typically 10 Å) on the right side of the molecule using the standard quantum mechanical definition of the current: $\mathbf{j}(\mathbf{r},t) = e\hbar/(2im)\sum_k^{N_{\text{occ}}}(\psi_k^*\nabla_{\mathbf{r}}\psi_k - \psi_k\nabla_{\mathbf{r}}\psi_k^*)$. We have observed that the emission current does not vary qualitatively (apart from a time shift due the difference in distance that the electrons must travel) as long as the plane is far from the molecule.

The total simulation times, in our calculations, were in the range of 20–25 fs. As mentioned above, the peak of the electric field oscillations was set to occur at the time $t = 5$ fs. After

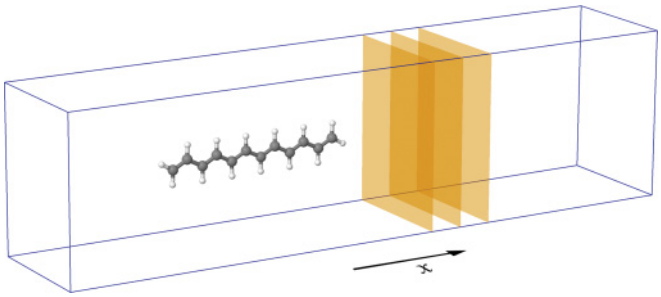

FIG. 2. (Color online) Simulation box containing a $C_{12}H_{14}$ molecule. Current is measured through planes behind the molecule. Beyond this, the complex absorbing potential acts.

that, the laser field oscillations gradually vanished and we observed the response of the system to the strong perturbation they had caused. Since the total simulation time of 20–25 fs is comparable to the vibrational period of a typical C–C or C–H bond, it is not immediately clear how significantly the motion of ions during that time could affect the current and whether that could qualitatively change the results. To check this, test calculations were performed by allowing the ions to move classically under the influence of quantum forces (i.e., Ehrenfest molecular dynamics). The ions were allowed to move only for the smallest system in our simulations, the $C_{12}H_{14}$ molecule. The motion of ions is described by the following system of equations:

$$M_i \frac{d^2\mathbf{R}_i}{dt^2} = -\nabla_{\mathbf{R}_i}\left[Z_i V_{\text{ext}}(\mathbf{R}_i,t) + \sum_{i<j}^{N_{\text{ion}}} \frac{Z_i Z_j}{|\mathbf{R}_i - \mathbf{R}_j|} + \int V_{\text{ion}}(\mathbf{r},\mathbf{R}_i) n(\mathbf{r},t) d\mathbf{r} \right], \quad (2)$$

which are coupled with the Kohn-Sham equation (1) through the electron density. In the above formula, M_i, Z_i, and $\mathbf{R}_i$ are the mass, (pseudo)charge, and the position, respectively, of the ith ion. Positions and velocities of the ions at each time step were calculated using the Verlet algorithm.

We first present our results for the linear $C_{12}H_{14}$ molecule, which serves as a simple model for a nanowire-like field emitter. We first optimized the geometry of the system in its ground state in order to avoid an artificial rearrangement of the ionic positions and a jump in the ionic temperature during the time evolution. The calculated currents are shown in Fig. 3. The plot has three curves, corresponding to the simulation with fixed ions, moving ions with zero initial temperature, and moving ions with the initial temperature of 300 K.

The calculated maximum currents due to the combined effect of laser pulse and static field, and due to static field only, are compared in Table I. These currents correspond to an emission of ~0.5% (static field plus laser) and 0.0006% (static field only) of the electrons. As discussed above, the static field is used to provide a preferred direction for the current, and produces only a small fraction of the observed current.

Figure 3 demonstrates that the laser pulse induces a current with a pulse-like pattern. As the top plot in Fig. 3 shows, the current starts to increase significantly at around 5 fs, which corresponds to the arrival of the Gaussian envelope peak, and then gradually decays. Notice the relatively long decay tail (significantly longer than the pulse duration). A possible explanation for this is that when the pulse arrives, electrons are excited to higher energies. These higher energies allow the electrons to tunnel out of the nanostructure at a higher rate, leading to a larger current. The current only returns to its prepulse levels once the excited electrons have tunneled out completely. Since the tunneling out can take longer than the initial transfer of energy from the pulse, a tail is observed on the emitted pulse.

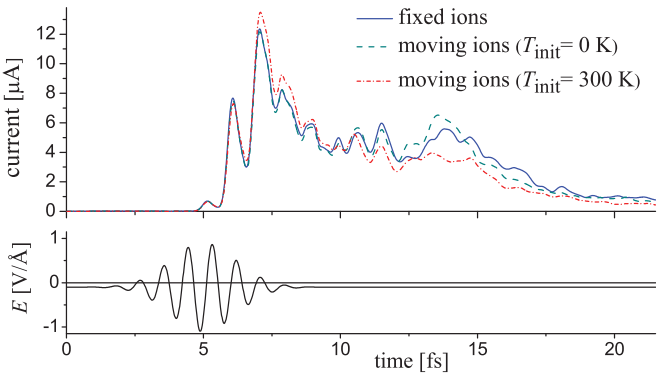

FIG. 3. (Color online) Ionization from a $C_{12}H_{14}$ molecule due to static electric and laser fields acting together (top) and the laser pulse as a function of time (bottom).

TABLE I. Maximum current values obtained with a static field of 0.1 V/Å only and with the static field and a laser pulse of 1.0 V/Å amplitude. All values are in μA.

	$C_{12}H_{14}$	(3,3) NT	(5,5) NT
Static field	0.01	0.04	0.03
Static field + laser pulse	12.4	20.3	45.9

The calculations have been repeated for segments of single walled (3,3) and (5,5) carbon nanotubes. Nanotubes are excellent field emitters that have been studied intensively both theoretically[30] and experimentally.[31–36] In the case of the (3,3) nanotube, we passivated dangling bonds with hydrogens. For the (5,5) case, we placed carbon caps at the ends. The total number of atoms in these systems was 84 and 120, respectively. The difference in current due to ionic motion was not expected to be significant (as simulations with $C_{12}H_{14}$ demonstrated), so the calculations used fixed ions.

The currents (see Table I) for the nanotubes look very similar (apart from an obvious change in the magnitude). Figure 4 shows results for the (5,5) case. Similar to $C_{12}H_{14}$, the current is several orders of magnitude higher when the laser is applied.

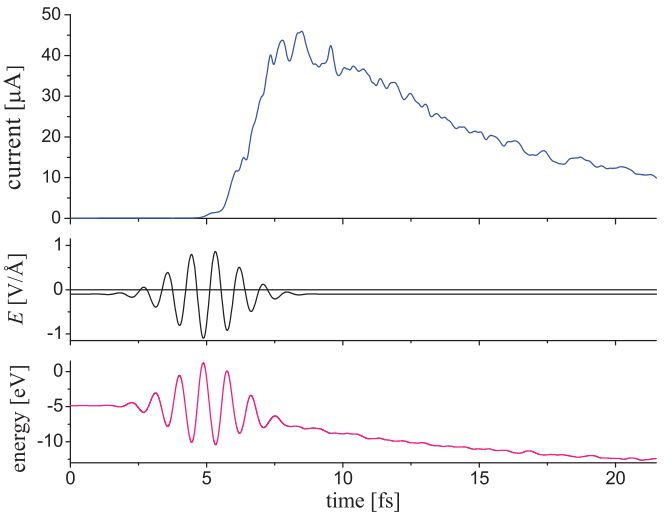

FIG. 4. (Color online) Ionization from a (5,5) carbon nanotube due to static electric and laser fields acting together (top) and the laser pulse as a function of time (middle). The bottom figure shows the energy of the highest occupied orbital.

The time-dependent change of the potential and the electron orbitals show that the ionization is due to the combined effect of electron excitation and a change in the potential barrier. The laser pulse excites the electrons that are close to the Fermi level and changes the shape of the potential that the electrons feel. The electron excitation changes the Hartree potential, further changing the potential barrier. Figure 4 shows energy of the highest occupied orbital as a function of time. The energy strongly oscillates due to the laser field in the duration of the pulse. After the laser pulse, the energy decreases due to the change in the electrostatic potential caused by the excitation of electrons.

In summary, we have used a first-principle approach to investigate the ionization of electrons from nanostructures induced by short intense laser pulses in the presence of a weaker uniform static field. Based on the results of our simulations, two important qualitative features of this process have been determined: (1) a significant enhancement of the current when a laser pulse is applied, and (2) the current has a peak of some duration and the position of this peak correlates with the time of the pulse arrival. These two features suggest the possibility of using short laser pulses for making few-electron emitters of nanoscale size.[5] Such emitters could have many desirable properties, especially very high spatial and time resolutions. To have a closer connection with experiments, these calculations should be extended to larger system. This would allow us to estimate the effect of the finite size (in lack of electron reservoir, limited number of electrons available for ionization) but this is beyond the current computational capabilities.

This work is supported by NSF Grant No. CMMI0927345.

[1]P. Hommelhoff, C. Kealhofer, and M. A. Kasevich, Phys. Rev. Lett. **97**, 247402 (2006).
[2]P. Hommelhoff, Y. Sortais, A. Aghajani-Talesh, and M. A. Kasevich, Phys. Rev. Lett. **96**, 077401 (2006).
[3]H. Yanagisawa, C. Hafner, P. Doná, M. Klöckner, D. Leuenberger, T. Greber, M. Hengsberger, and J. Osterwalder, Phys. Rev. Lett. **103**, 257603 (2009).
[4]W. E. King, G. H. Campbell, A. Frank, B. Reed, J. F. Schmerge, B. J. Siwick, B. C. Stuart, and P. M. Weber, J. Appl. Phys. **97**, 111101 (2005).
[5]H. Niikura, F. Legare, R. Hasbani, A. Bandrauk, M. Ivanov, D. Villeneuve, and P. Corkum, Nature **417**, 917 (2002).
[6]J. Lin, N. Weber, A. Wirth, S. Chew, M. Escher, M. Merkel, M. Kling, M. Stockman, F. Krausz, and U. Kleineberg, J. Phys. Condens. Matter **21**, 314005 (2009).
[7]M. Schnürer, C. Spielmann, P. Wobrauschek, C. Streli, N. H. Burnett, C. Kan, K. Ferencz, R. Koppitsch, Z. Cheng, T. Brabec, and F. Krausz, Phys. Rev. Lett. **80**, 3236 (1998).
[8]C. A. Brau, Nucl. Instrum. Methods A **407**, 1 (1998).
[9]S. Grafström, J. Appl. Phys. **91**, 1717 (2002).
[10]L. Keldysh, Sov. Phys. JETP **20**, 1307 (1965).
[11]P. L. Shkolnikov, A. E. Kaplan, and S. F. Straub, Phys. Rev. A **59**, 490 (1999).
[12]A. E. Kaplan, B. Y. Dubetsky, and P. L. Shkolnikov, Phys. Rev. Lett. **91**, 143401 (2003).
[13]I. Last and J. Jortner, J. Chem. Phys. **121**, 8329 (2004).
[14]V. F. Kovalev, K. I. Popov, V. Y. Bychenkov, and W. Rozmus, Phys. Plasmas **14**, 053103 (2007).
[15]X. Chu and M. McIntyre, Phys. Rev. A **83**, 013409 (2011).
[16]J. Muth-Böhm, A. Becker, and F. H. M. Faisal, Phys. Rev. Lett. **85**, 2280 (2000).
[17]S. Petretti, Y. V. Vanne, A. Saenz, A. Castro, and P. Decleva, Phys. Rev. Lett. **104**, 223001 (2010).
[18]E. Runge and E. K. U. Gross, Phys. Rev. Lett. **52**, 997 (1984).
[19]T. Otobe, K. Yabana, and J.-I. Iwata, J. Phys. Condens. Matter **21**, 064224 (2009).
[20]T. Otobe and K. Yabana, Phys. Rev. A **75**, 062507 (2007).
[21]M. Lein, E. K. U. Gross, and V. Engel, Phys. Rev. A **64**, 023406 (2001).
[22]M. Isla and J. A. Alonso, Phys. Rev. A **72**, 023201 (2005).
[23]Y. Kawashita, T. Nakatsukasa, and K. Yabana, J. Phys. Condens. Matter **21**, 064222 (2009).
[24]E. Livshits and R. Baer, J. Phys. Chem. A **110**, 8443 (2006).
[25]A. Castro, M. Marques, J. Alonso, G. Bertsch, and A. Rubio, Eur. Phys. J. D **28**, 211 (2004).
[26]J. P. Perdew and A. Zunger, Phys. Rev. B **23**, 5048 (1981).
[27]N. Troullier and J. L. Martins, Phys. Rev. B **43**, 1993 (1991).
[28]G. Halasz and A. Vibok, Int. J. Quantum Chem. **92**, 168 (2003).
[29]D. Manolopoulos, J. Chem. Phys. **117**, 9552 (2002).
[30]J. A. Driscoll and K. Varga, Phys. Rev. B **80**, 245431 (2009).
[31]W. de Heer, A. Châtelain, and D. Ugarte, Science **270**, 1179 (1995).
[32]J. Bonard, J. Salvetat, T. Stöckli, W. de Heer, L. Forró, and A. Châtelain, Appl. Phys. Lett. **73**, 918 (1998).
[33]N. de Jonge, Y. Lamy, K. Schoots, and T. Oosterkamp, Nature **420**, 393 (2002).
[34]K. Teo, E. Minoux, L. Hudanski, F. Peauger, J. Schnell, L. Gangloff, P. Legagneux, D. Dieumegard, G. Amaratunga, and W. Milne, Nature **437**, 968 (2005).
[35]A. G. Rinzler, J. H. Hafner, P. Nikolaev, P. Nordlander, D. T. Colbert, R. E. Smalley, L. Lou, S. G. Kim, and D. Tomanek, Science **269**, 1550 (1995).
[36]J.-M. Bonard, K. A. Dean, B. F. Coll, and C. Klinke, Phys. Rev. Lett. **89**, 197602 (2002).